

Perspectives on Multi-Level Dynamics

Fatihcan M. Atay^{*} Sven Banisch[†] Philippe Blanchard[‡] Bruno Cessac[§]
Eckehard Olbrich[¶] Dima Volchenkov^{||}

June 7, 2022

Abstract

As Physics did in previous centuries, there is currently a common dream of extracting generic laws of nature in economics, sociology, neuroscience, by focalising the description of phenomena to a minimal set of variables and parameters, linked together by causal equations of evolution whose structure may reveal hidden principles. This requires a huge reduction of dimensionality (number of degrees of freedom) and a change in the level of description. Beyond the mere necessity of developing accurate techniques affording this reduction, there is the question of the correspondence between the initial system and the reduced one. In this paper, we offer a perspective towards a common framework for discussing and understanding multi-level systems exhibiting structures at various spatial and temporal levels. We propose a common foundation and illustrate it with examples from different fields. We also point out the difficulties in constructing such a general setting and its limitations.

1 Introduction

It is generally agreed that complex systems are comprised of a large number of sub-components and their interactions. Moreover, they often exhibit structures at various spatial and temporal levels. As a somewhat extreme example, spanning length and time scales of vastly different magnitudes, one can cite the hierarchy of molecules, neurons, brain areas, brains, individuals, social organizations, economies, etc., which can be viewed as manifestations of the same collective physical reality at different levels. Scientific disciplines like biology, neuroscience, psychology, sociology, economy, and so on, have typically evolved based on notions and descriptions relevant for a certain level. Nevertheless, even within a single discipline it is sometimes desirable to distinguish and investigate several levels and their interactions, such as in the fields of macro and micro economics. It is

^{*}Max Planck Institute for Mathematics in the Sciences, D-04103 Leipzig, Germany. atay@member.ams.org

[†]Max Planck Institute for Mathematics in the Sciences, D-04103 Leipzig, Germany. sven.banisch@universecity.de

[‡]University of Bielefeld, Department of Physics D-33619 Bielefeld, Germany. philippe.blanchard@uni-bielefeld.de

[§]Inria Sophia Antipolis Méditerranée, Neuromathcomp project-team, Sophia Antipolis 06902, France. bruno.cessac@inria.fr

[¶]Max Planck Institute for Mathematics in the Sciences, D-04103 Leipzig, Germany. olbrich@mis.mpg.de

^{||}University of Bielefeld, Center of Excellence - Cognitive Interaction Technology (CITEC), D-33619 Bielefeld, Germany. volchenk@physik.uni-bielefeld.de

therefore a question of both theoretical and practical interest how different descriptions of the same large system at various levels are related to each other.

In this paper, we offer some perspectives towards a common framework for discussing and understanding multi-level systems. Since we cannot hope to address the generality of systems from every area of science, for the presentation we have chosen a few important fields to exemplify the main ideas. These are information theory (Section 2), Markov chains and agent-based models (Section 3), mean-field methods in neuroscience (Section 4), renormalization group theory (Section 5), and quantum decoherence (Section 6). As these examples are very different from each other, we shall use this introductory section to form a connecting foundation. The main idea can be graphically illustrated in the diagram of Figure 1, which will be at the basis of the discussion in the following sections and will be amended and generalized in various ways.

When we talk about a *system*, we are referring to a *dynamical system*, namely, there is an underlying *state space* X as well as a rule ϕ for transition between states. This aspect is represented in the horizontal direction in Figure 1. The function ϕ describes the time evolution in discrete time (such as iteration-based rules like Markov chains) or in continuous time (such as the solution operator or flow of a differential equation), mapping the current state of the system to a future state. The diagram can be replicated in the horizontal direction to correspond to the time trajectory of the system.

The vertical direction of Figure 1, on the other hand, corresponds to the *levels* of the system. Here, one can conceive of another state space Y which describes the system using a different set of variables. The function π in the diagram represents the passage from one set of variables to another. Probably the foremost striking feature in the hierarchy of levels is the (usually huge) difference in the number of variables, i.e., the degrees of freedom, that are used for the description of the system. Hence, for our purposes, π is *not* a coordinate transformation; in fact, it is many-to-one, although it can be assumed to be surjective with no loss of generality. Correspondingly, one can then refer to the elements of X and Y as micro and macro variables, respectively. Such operators as π have been studied in the literature under the more or less related names of *aggregation*, *reduction*, *projection*, *coarse-graining*, or *lumping*. For instance, π may describe a grouping of several variables into one, which would relate it to the aggregation operation in Markov chains (see Section 3), or it may be a simple averaging operation of the system variables, which would relate it to the *mean-field* methods of reduction (see Section 4). The diagram can be repeated in the vertical direction to describe a hierarchy of multiple levels in the system.

The main thread of our discussion hinges upon the question whether the horizontal and vertical directions in Figure 1 can be reconciled in some sense. Formally, this happens if there exists a function $\psi : Y \rightarrow Y$ such that the diagram commutes, that is $\pi\phi = \psi\pi$. If that is the case, then ψ provides a description of the time evolution of the system using only the Y variables. In other words, the macro variables of Y afford a closed and independent description of the system, at least as far as its dynamical evolution is concerned; and hence we formally view Y as a *level* in the system. The conditions for Y to constitute a level thus depends on the properties of the dynamics ϕ and the reduction operator π . Such conditions have been derived for several classes of systems; for more details, the interested reader is referred to the recent preprints [3, 26] and the references therein.

At this point perhaps some comments on terminology are in order, since there are variations in usage in different fields. In this paper, we distinguish between the concepts of *scales* and *levels*. Broadly speaking, we view scales as being essentially related to the measurement process and the representation of observed data at different resolutions.

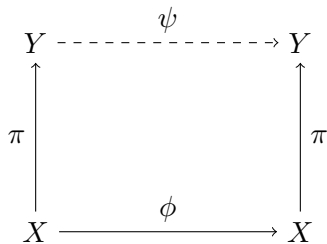


Figure 1: Schematic view of a multi-level dynamical system.

In contrast, we characterize a level by the fact that it admits a closed functional description in terms of concepts and quantities intrinsic to that level, at least to a certain degree of approximation. Thus, when focusing at a particular level, the system function is described and explained in terms of concepts specific to a certain view on the system. The distinction of terminology, while not standard in every field, will be important for elucidating the upcoming discussion.

The perspectives about multi-level structures that will be discussed in the following pages can essentially be traced to different ways of interpreting the commutativity of the diagram in Figure 1. In fact, an important case is when the diagram does *not* commute for given (ϕ, π) , at least not exactly. This naturally leads to the concept of *approximately closed* levels and one is then interested in quantifying the discrepancy in terms of *closure measures*. For instance, in normed spaces the difference $\|\pi\phi - \psi\pi\|$, or more precisely,

$$\delta = \sup_{x \in \mathcal{A}} \|\pi(\phi(x)) - \psi(\pi(x))\| \quad (1)$$

where $\mathcal{A} \subseteq X$ is some subset of states of interest, would be such a measure. Other measures based on an information-theoretic point of view will be discussed in Section 2.

The lack of exact commutativity can manifest itself in various ways in the description of the system at the macro level Y . In some instances, one has to deal with *memory effects*, as discussed in Section 3, which may require that the state space Y be appropriately extended to obtain a well-defined dynamical system at the macro level. In other cases, the loss of information about the exact state of the system, caused by the many-to-one nature of the mapping π , may typically lead to stochasticity in the description ψ even if the micro-level dynamics ϕ is completely deterministic. However, the converse effect is also possible, as the stochastic effects that may be present at the micro level may be averaged out by the mapping π , leading to *less* stochasticity at the macro level, even converging to a deterministic description in appropriate limits. Such a limiting behavior can be visualized by referring to a sequence of diagrams such as Figure 1. For instance, let ϕ_n describe the dynamics of an n -dimensional system on the state space $X_n = \mathbb{R}^n$, let $\pi_n : \mathbb{R}^n \rightarrow \mathbb{R}$ be the averaging operator, and $Y = \mathbb{R}$. The discrepancy measure given in (1), namely $\delta_n = \|\pi_n \phi_n - \psi \pi_n\|$, may be nonzero for each n but we may have $\delta_n \rightarrow 0$ in the limit as the system size $n \rightarrow \infty$. Section 4 discusses this aspect in detail in the context of mean field equations.

Finally, we consider the two examples of multi-level systems where dynamics is specified without reference to a particular equation of motion. In Section 5, any trace of certain dynamical evolution is absent from consideration, as only the final, “steady state” is of interest (as under the entropy maximization and least efforts principles). The coarse-grained, multi-level representation here aims at improving the analytical properties of

perturbation theory. We work with the generalized scaling degrees of freedom—in which time and space are not explicitly distinguished against each other—instead of the physical degrees of freedom discussed in the other sections. The scaling degrees of freedom are related to the physical degrees of freedom of the original model by means of the Renormalization Group transformations and thus enjoy a renormalization group structure, a kind of symmetry that might facilitate their investigation. Section 6 considers the problem of quantum decoherence, in which the multi-level description has the quantum and classical representation, and the "quantum level" degrades to the classical one in infinite time.

2 Information theoretic approach to multilevel systems

In this section we will provide an information theoretic analysis of multi-level systems as represented in the diagram Fig. 1. We will study, how the information flow within the levels is related to the information flow between the levels and to the existence of closed descriptions within a level.

In order to so we will consider the following setting:

- The microscopic state at time t is described by a random variable X_t with discrete states $x \in \mathcal{X}$
- The macroscopic state at time t is described by a random variable Y_t with discrete states in $y \in \mathcal{Y}$.
- The macrostate y is determined by the microstate via a stochastic map $\pi : X \rightarrow Y$ representing the aggregation, projection or some other reduction operation. Thus, the choice of π defines the macroscopic *level* Y .
- The microscopic dynamics ϕ is a discrete time dynamics and assumed to be Markov chain with $\phi(x_{t+\tau}|x_t)$ denoting the conditional probability that the system is at time $t + \tau$ in state $x_{t+\tau}$ given that it was in state x_t at time t .
- As macroscopic dynamics ψ we consider the dynamics "induced" by the π and ϕ in the sense that

$$\begin{aligned} \psi(y_{t+\tau}|y_t) &:= p(y_{t+\tau}|y_t) \\ &= \frac{\sum_{x_t \in \mathcal{X}} \sum_{x_{t+\tau} \in \mathcal{X}} \pi(y_{t+\tau}|x_{t+\tau}) \phi(x_{t+\tau}|x_t) p(x_t)}{\sum_{x_t \in \mathcal{X}} \pi(y_t|x_t) p(x_t)} \end{aligned}$$

- With these definitions the diagram in Fig. 6 can be read as a Bayesian network which means that the joint probability distribution factorizes as follows

$$p(y_{t+\tau}, y_t, x_{t+\tau}, x_t) = \pi(y_{t+\tau}|x_{t+\tau}) \phi(x_{t+\tau}|x_t) \pi(y_t|x_t) p(x_t) . \quad (2)$$

Here we made the assumption that the microscopic state provides a complete description in the sense that the dynamics on the microlevel is Markovian, which is a common requirement for defining the "state" of system. However, for the sake of simplicity we have additionally restricted ourselves to discrete states and time discrete dynamics.

For the information theoretic analysis we need the following quantities (for a more detailed treatment see for instance [18]):

The Shannon entropy

$$H(X) = - \sum_{x \in \mathcal{X}} p(x) \log p(x)$$

provides a measure for the uncertainty of the outcome of measuring the random variable X . The conditional entropy

$$\begin{aligned} H(X|Y) &= - \sum_{x \in \mathcal{X}, y \in \mathcal{Y}} p(x, y) \log p(x|y) \\ &= H(X, Y) - H(Y) \end{aligned}$$

quantifies the remaining average uncertainty if one knows already the value of Y . By already knowing Y the uncertainty of X is reduced by the information that is provided by Y , therefore the *mutual information* between X and Y is the difference the entropy $H(X)$ and the conditional entropy $H(X|Y)$:

$$I(X; Y) = H(X) - H(X|Y) \quad (3)$$

With the same argument one can also introduce the *conditional mutual information* as the information that Y provides about X , if a third variable Z is already known:

$$I(X; Y|Z) = H(X|Z) - H(X|Y, Z) \quad (4)$$

The microdynamics being Markovian means that the future state $X_{t+\tau}$ is conditionally independent from the past $X_{t-\tau}, X_{t-2\tau}, \dots$ given the present state X_t . This is equivalent to a vanishing of conditional mutual information

$$I(X_{t+\tau}; X_{t-\tau}, X_{t-2\tau}, \dots | X_t) = 0.$$

Thus, the information flow in the lower level is completely characterized by the mutual information of two consecutive time steps $I(X_t; X_{t+\tau})$. In order to see which part of this information can be observed also in the upper level we start from the joint mutual information of the lower and upper level $I(X_{t+\tau}, Y_{t+\tau}; X_t, Y_t)$ and apply the chain rule. The factorization of the joint probability Eq. (2) implies the conditional independences

$$X_{t+\tau} \perp\!\!\!\perp Y_t | X_t \quad Y_{t+\tau} \perp\!\!\!\perp (X_t, Y_t) | X_{t+\tau}$$

A simple way to see this is verifying the corresponding d-separation property [23] in the Bayesian network. Using that the corresponding conditional mutual informations $I(X_{t+\tau}; Y_t | X_t) = 0$ and $I(Y_{t+\tau}; X_t, Y_t | X_{t+\tau}) = 0$ vanish one arrives at the following result:

$$\begin{aligned} I(X_{t+\tau}; X_t) &= I(Y_{t+\tau}; Y_t) + I(Y_{t+\tau}; X_t | Y_t) \\ &\quad + I(X_{t+\tau}; Y_t | Y_{t+\tau}) + I(X_{t+\tau}; X_t | Y_{t+\tau}, Y_t) \end{aligned} \quad (5)$$

The single terms on the right side have a clear interpretation:

$I(Y_{t+\tau}; Y_t)$: Information between two successive steps on the macrolevel. This is part of the information flow in the macrolevel. However, in contrast to the microlevel the macrolevel is not necessarily Markovian and therefore there could be additional contributions to the information flow within this level which we will discuss below.

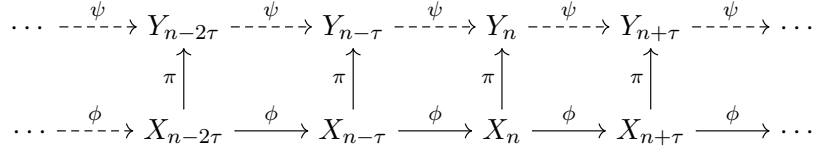


Figure 2: Bayesian network of the multilevel system for several consecutive time steps.

$I(Y_{t+\tau}; X_t | Y_t)$: Information flow from the micro- to the macrolevel. If this term is non-zero, knowing the micro-state will provide additional information about the future value of the macrostate given that one knows the current value of the macrostate. On the contrary, if this conditional mutual information vanishes, we will say that the macrolevel is **informational closed**. In fact, as we will show below, informational closure implies Markovianity of the macrolevel [34], but not vice versa, see [33] for an example.

$I(Y_t; X_{t+\tau} | Y_{t+\tau})$: This is also an information flow between the micro- and the macrolevel, but in contrast to the previous one, backwards in time. Here one asks whether knowing the microstate will provide additional information about the previous macrostate which is not known from the current macrostate. While the previous flow is related to information production on the macrolevel, that is which part of the macroscopic randomness can be explained by microscopic determinism, here one deals with the information destruction on the macrolevel and asks whether some of this information survived on the microlevel.

$I(X_{t+\tau}; X_t | Y_{t+\tau}, Y_t)$ This term contains the part of the microscopic information flow that is irrelevant for the macrodynamics.

So far we studied only information flows within a single time step. However, the dynamics on the macrolevel can be Non-Markovian and it is natural to ask, how this Non-Markovianity is related to the information within the macrolevel. Therefore, we extend the basic diagram Fig. 1 and consider more time steps. We will use the following notation: $X_{t-n\tau}^t = (X_t, X_{t-\tau}, \dots, X_{t-n\tau})$. In particular, $X_{-\infty}^t$ will denote the complete past.

Then the dynamics on the macro-level is Non-Markovian if and only if the conditional mutual information

$$I(Y_{t+\tau}; Y_{-\infty}^{t-\tau} | Y_t) \neq 0 .$$

On the other hand we assumed that the micro-dynamics is Markovian and therefore

$$I(X_{t+\tau}; X_{-\infty}^{t-\tau} | X_t) = 0 .$$

Applying the chain rule to the conditional mutual information $I(Y_{t+\tau}; X_t, Y_{-\infty}^{t-\tau} | Y_t)$ and using the conditional independence $I(Y_{t+\tau}; Y_{-\infty}^{t-\tau} | X_t, Y_t) = 0$ yields the following identity:

$$I(Y_{t+\tau}; X_t | Y_t) = I(Y_{t+\tau}; Y_{-\infty}^{t-\tau} | Y_t) + I(Y_{t+\tau}; X_t | Y_{-\infty}^t)$$

This identity has the following implication: The forward information flow between the micro- and macrolevel provides an upper bound for the Non-Markovianity of the macrolevel

$$I(Y_{t+\tau}; X_t | Y_t) \geq I(Y_{t+\tau}; Y_{-\infty}^{t-\tau} | Y_t) \quad (6)$$

One consequence of this fact is that a vanishing information flow, i.e. *informational closure*, implies Markovianity (i.e. lumpability, see next section) on the macro-level.

3 Lumpability in Agent-Based Models

We continue these considerations by applying concepts of the previous sections to a class of models referred to as agent-based models. In addition to the information-theoretic measures we will focus on the concept of lumpability in Markov chain theory which makes statements about the possibility to aggregate the states of a Markov chain such that the process projected onto that aggregated state space is still a Markov chain. We start with a description of the microscopic dynamics of a class of agent-based models.

3.1 A class of agent-based models as Markov chains

Agent-based models aim at describing certain societal phenomena by putting individual actors (the agents) into a virtual environment, specifying simple rules of how these agents interact and letting the system evolve to observe the macroscopic outcomes of the individual interactions. A famous example is Schelling's model of spatial segregation [35] which shows that a population of agents with a slight preference of settling close to agents of a similar kind produces macroscopic patterns of spatial segregation. Another often-cited example is the Axelrod model of cultural dissemination [4] emphasizing that a similar mechanism of similarity-driven interaction can provide an explanation for the stable co-existence of populations with different cultural traits. These models are usually implemented as a computer program and extensive simulation experiments are performed to understand the global outcome of these high-dimensional systems of heterogeneous interacting agents.

Let us consider here a class of models where N agents can be in δ different states. Consider further that the agent states are updated sequentially such that from one time step to the other, an agent i is chosen at random along with another agent j . The probability of choosing an agent pair (i, j) , denoted here as ω_{ij} , is determined by a weighted interaction network W which defines the neighborhood structure of the agent population. For instance, the case that two agents are chosen merely at random is encoded by the complete graph $W = K_N$ and the corresponding probability of choosing a pair (i, j) is $\omega_{ij} = 1/N(N-1)$ for all $i \neq j$. This particular case is sometimes referred to as homogeneous mixing or random mating, depending on the application context.

We consider the case that at one time¹ step t a single agent pair (i, j) is chosen and only agent i changes its state in dependence of its own current state $x_i(t)$ and the current state of the neighbor $x_j(t)$ by a local update rule

$$x_i(t+1) = u(x_i(t), x_j(t)). \quad (7)$$

This allows us to specify the microscopic transition probabilities between all possible system configurations $x = (x_1, \dots, x_n) \in \{1, \dots, \delta\}^N$. Namely, under sequential update only one agent (i) may change at a time giving rise to a transition $x \xrightarrow{i} x'$ such that $x_i \neq x'_i$ and $x_k = x'_k, \forall k \neq i$. The transition probability for $x \xrightarrow{i} x'$ is then given by

$$\phi(x'|x) = \sum_{j:(x'_i, x'_j)=u(x_i, x_j)} \omega_{ij}. \quad (8)$$

Under this assumptions, it is easy to show that the micro-level dynamics of such a model can be viewed as a set of random walkers on the Hamming graph $H(N, \delta)$ (with loops).

¹Notice that we use the convention that time indices are in the brackets and the subscript is the agent index. We also say that the process has evolved to time $t+1$ after each interaction event.

Hamming graphs are a class of distance-regular graphs in which the nodes are defined as all N -tuples of symbols from an alphabet $\{1, \dots, \delta\}$ and links exist between nodes with a Hamming distance of one. In our case, the state space of the micro chain is defined by the set of all possible configurations of agents $x = (x_1, \dots, x_i, \dots, x_N)$ with $x_i \in \{1, \dots, \delta\}$ and under sequential update by (7) at most one position in the configuration can change from one time step to the next.

As we will see in the next section, the rather regular structure of the micro chain associated to an agent-based simulation model is rather useful for establishing cases in which the macroscopic dynamics induced by ϕ and π are Markovian. For this purpose, we next describe the lumpability concept.

3.2 Lumpability

Let us restate the (strong) lumpability Theorem 6.3.2 from [28]. Let $p(Y|x) = \sum_{x' \in Y} \phi(x'|x)$ denote the conjoint probability for $x \in \mathcal{X}$ to go to the set of elements $x' \in Y$ where $Y \subseteq \mathcal{X}$ is a subset of the configuration space which several micro states are lumped (aggregated) to.

Theorem 3.1 ([28]:124) *A necessary and sufficient condition for a Markov chain to be lumpable with respect to a partition $\mathcal{Y} = (Y_1, \dots, Y_r)$ is that for every pair of sets Y_i and Y_j , $p(Y_j|x)$ have the same value for every x in Y_i . These common values $\{p_{ij}\}$ form the transition matrix for the lumped chain.*

In general it may happen that, for a given Markov chain, some projections are Markov and others not. As different macroscopic properties correspond to different partitions \mathcal{Y} on which the micro process is projected, this also means that it depends on the system property at question whether the time evolution at the associated level of observation is Markovian or not.

On the basis of this Theorem, we have derived in [8] a sufficient condition for lumpability which makes use of the symmetries of the chain:

Theorem 3.2 *Let (\mathcal{X}, ϕ) be a Markov chain and $\mathcal{Y} = (Y_1, \dots, Y_r)$ a partition of \mathcal{X} . For any partition there exists a group \mathcal{G} of bijections on \mathcal{X} that preserve the partition ($\forall x \in Y_i$ and $\forall \sigma \in \mathcal{G}$ we have $\sigma(x) \in Y_i$). If the Markov transition probability matrix ϕ is symmetric with respect to \mathcal{G} ,*

$$\phi(x'|x) = \phi(\sigma(x')|\sigma(x)) : \forall \sigma \in \mathcal{G}, \quad (9)$$

the partition (Y_1, \dots, Y_r) is (strongly) lumpable.

As an example, let us consider the Land of Oz Markov chain repeatedly considered in [28] (Example 6.4.2). The idea is that the weather in the Land of Oz is described by the transition probabilities between three different weather states ("Sun", "Rain" and "Snow") as follows

$$\phi = \begin{array}{c} \text{Sun} \\ \text{Rain} \\ \text{Snow} \end{array} \left(\begin{array}{c|cc} 0 & \frac{1}{2} & \frac{1}{2} \\ \hline \frac{1}{4} & \frac{1}{2} & \frac{1}{4} \\ \hline \frac{1}{4} & \frac{1}{4} & \frac{1}{2} \end{array} \right) \xrightarrow{\text{(strong lump)}} \psi = \begin{array}{c} \text{Nice} \\ \text{Bad} \end{array} \left(\begin{array}{cc} 0 & 1 \\ \frac{1}{4} & \frac{3}{4} \end{array} \right)$$

An example for a lumpable partition for this chain is given by the aggregation π of the states "Rain" and "Snow" into a macro state "Bad" weather. The conditions of 3.1 are satisfied as the transition probabilities from the "Rain" and "Snow" to the lumped state

$\{\text{Rain}, \text{Snow}\}$ as well as to $\{\text{Sun}\}$ are equal. Moreover, this example is also suited to illustrate Theorem 3.2. Namely, it is easy to see that permuting the states "Rain" and "Snow" does not change the transition matrix ϕ .

3.3 Application to agent-based models

Theorem 3.2 is particularly interesting for agent-based models because it relates the question of lumpability to the *automorphisms* of the micro chain ϕ and the structure (or "grammar") $H(N, \delta)$ is known to possess many automorphisms. In fact, interpreting ϕ as a weighted graph, the symmetry relation (9) is precisely the usual definition of a graph automorphism. The set of all permutations σ that satisfy (9) corresponds then to the automorphism group of (\mathcal{X}, ϕ) and Theorem 3.2 states that this group can be used to define a lumpable partition.

Now, the automorphism group of the Hamming graph $H(N, \delta)$ is given by the semi-direct product $\mathcal{S}_\delta \rtimes \mathcal{S}_N$ [25] where the second component accounts for permutation invariance with respect to the agents and the first for symmetries with respect to the δ possible agent attributes. For a model that realizes all these symmetries such that $\phi(x'|x) = \phi(\sigma(x')|\sigma(x))$ for all $\sigma \in \mathcal{S}_\delta \rtimes \mathcal{S}_N$, the full automorphism group of $H(N, \delta)$ is realized and this allows for a reduction from a micro chain of size δ^N to a macro chain with $N/2$ (for even N) or $(N+1)/2$ (for odd N) states [5] – a quite considerable reduction.

However, the transition probabilities as specified in (8) satisfy complete permutation invariance with respect to the agents only in the rather particular case of homogeneous mixing where the probabilities ω_{ij} of choosing agent pair (i, j) is equal for all pairs. Likewise, the permutability of all agent states $\{1, \dots, \delta\}$ hinges on an update rule u that is unbiased with respect to the different state pairings meaning essentially that exactly the same rule must be used for all pairs of states. For instance, any dependence or constraint on the distance between x_i, x_j such as assortative mating in population genetics or bounded confidence in opinion dynamics do violate some of these symmetries and, in fact, lead to more interesting macroscopic outcome for this reason.

Therefore, as soon as constraints are implemented in a model (and a model without any constraints is often not that interesting) certain irregularities will appear in the micro chain which reduces the number of automorphisms and require therefore a refinement of the macroscopic partition. Interestingly, we can relate constraints due to an heterogeneous interaction graph W and constraints on the rules u independently to the resulting automorphisms of ϕ . Namely, let $\mathcal{S}_\omega \subset \mathcal{S}_N$ denote the automorphisms of W and $\mathcal{S}_u \subset \mathcal{S}_\delta$ the remaining symmetries of the δ states under u , then the automorphism group of ϕ is $\mathcal{G} = \mathcal{S}_u \rtimes \mathcal{S}_\omega$. The problem of finding a group \mathcal{G} that can be used to construct a lumpable partition by Theorem 3.2 is therefore reduced to identifying the symmetries of the interaction graph W and the symmetries between the δ possible states under the update rule u whereas most other approaches to lumpability require the analysis of the δ^N -dimensional micro chain ϕ . See [7] for details and an application to the voter model.

The following conclusions can be drawn:

1. *The more constrained and heterogeneous the microscopic interaction probabilities and rules, the more irregular the micro process and the lower the chances to obtain a reasonable reduction by lumpability.*
2. *An observation function $\pi : \mathcal{X} \rightarrow \mathcal{Y}$ will define a lumpable macro process only if it is compatible with the symmetries of the micro chain.*

3. *If we decide to stay at the macro level despite the fact that it is not compatible with the symmetries of the micro chain, the macro process is no longer Markovian and non-Markovian memory is introduced at the macro level.*

To illustrate some of these results we will finalize this section with an example.

3.4 Emergence of memory effects

The presence of non-trivial temporal correlations is an important empirical fingerprint of data series produced by complex systems. Lumpability applied to agent-based models makes clear that Markovian macro dynamics can be expected only in exceptional cases. Far more generally, Markovianity is lost at an aggregate level and a crucial role in this is played by the microscopic heterogeneity implemented in the agent model, the nature of the correlations due to the underlying structure and the constraints in the interaction rules. For a better understanding of the contribution of these factors, we envision that lumpability can be combined with the information-theoretic framework for the quantification of "closure" described in Section 2. In order to better understand the temporal patterns that emerge in the transition from a microscopic model with heterogeneous agents to the macroscopic descriptions of practical interest, the Markovianity measure and information flow (related by (6)) are of particular interest.

For computing information flow and Markovianity for a micro level Markov chain \mathcal{X}, ϕ corresponding to an agent-based model and an induced macro-level process \mathcal{Y}, ψ we have to deal with the fact that the size of the micro chain is huge and that the direct computation of these information measures will often be unfeasible. One way to deal with this is to first use the symmetries of the micro model ($\mathcal{S}_u \rtimes \mathcal{S}_\omega$) and derive a lumpable meso-level description using Theorem 3.2. In Figure 3 this first projection is referred to as $\tilde{\pi}$ and the associated mesoscopic state space is denoted by $\tilde{\mathcal{X}}$. Since the Markov chain derived for the dynamics at this intermediate level is loss-less with respect to the original micro dynamics, the information quantities involved in the computation of the closure measures can be computed using the reduced-size meso-level chain $(\tilde{\mathcal{X}}, \tilde{\phi})$.

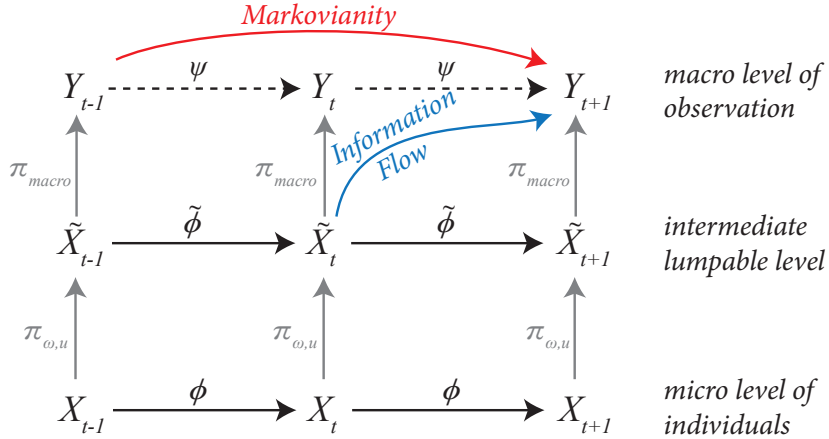


Figure 3: Information flow and Markovianity can be computed on the basis of an intermediate meso-level description that complies with $\mathcal{S}_u \rtimes \mathcal{S}_\omega$.

This process is particularly applicable to structured populations where a number of homogeneous communities is arranged as a chain or on a lattice. As an example, we shall

consider a voter model on a two-community graph consisting of two homogeneously coupled populations (a and b) with strong connections within the sub-populations and weak links connecting the individuals from different populations. This setup is very similar to the multi-population model of neuronal dynamics dealt with in the next section. We define the interaction network W as $\bar{W}_{aa} = \bar{W}_{bb} = 1$ meaning that two agents within the same population a or b are linked with weight 1, and $\bar{W}_{ab} = \bar{W}_{ba} = r$ which, to encode weak ties, is assumed to be smaller than one.

In the model, there are N agents with binary states, $x_i \in \{0, 1\}$. If an agent pair (i, j) is chosen – and this happens with a probability ω_{ij} proportional to W_{ij} – we say that agent i *imitates* the state of j with probability $1 - p$ and adopts the *contrarian* view with probability p . Notice that for $p = 0$ this corresponds to the voter model.

For binary agent, the microscopic state space is the set of all bit-strings of length N and the graph associated to the micro-level dynamics is the Hamming graph $H(N, 2)$, that is: the N -dimensional hypercube. Most typically, the system observable in this type of models is the number of agents in state 1 given by $k = \sum_{i=1}^N x_i$ also called Hamming weight. However, due to the inhomogeneity introduced by the fact that not all agent pair are chosen with equal probability (for $\bar{W}_{aa} \neq \bar{W}_{ab}$) the projection onto this partition is not lumpable.

However, in this stylized model, the structure of W is such that it is permutation invariant with respect to permutations of agents within the same sup-population so that a lumpable description is obtained by tracking independently the number of agents in state 1 in the two sub-populations, $k_{a(b)} = \sum_{i \in a(b)} x_i$. Let $N_{a(b)}$ denoting the number of agents in the two populations, then the state space of this lumped chain is $\tilde{\mathcal{X}} = \{\tilde{x}_{k_a, k_b} : 0 \leq k_a \leq N_a, 0 \leq k_b \leq N_b\}$ which is of size $N_a + 1 \times N_b + 1$. It is also clear that this state space is a refinement of the macroscopic partition as $k_a + k_b = k$.

Therefore, on the basis of the meso chain $(\tilde{\mathcal{X}}, \tilde{\phi})$ derived for the two-community case, we can exactly compute² the information flow $I(Y_{t+1}; X_t | Y_n) = I(Y_{t+1}; \tilde{X}_t | Y_n)$ from the lower to higher level and Markovianity measures for finite histories with $I(Y_{n+1} : Y_{n-1} | Y_n) \leq I(Y_{n+1} : Y_{n-1}, Y_{n-2} | Y_n)$. We show this for a system with $N_a = N_b = 50$ in Figure 4. The information flow is shown in red and the Markovianity in orange (one step into the past) and blue (two steps into the past) as a function of the ratio r between weak and strong ties (l.h.s) and the contrarian rate p (r.h.s.). On the r.h.s. three representative macroscopic realizations of the model are shown to give an idea of the model dynamics. Notice that the measures vanish in the absence of inhomogeneities ($r = 1$) as shown in the inset on the l.h.s. Notice also that the information flow from micro to macro is larger than the finite-history Markovianity measure as predicted by (6).

This demonstrates that the information-theoretic measures described in Section 2 constitute promising tools to study the relationship between different levels agent-based models. Global aggregation over an agent population without sensitivity to micro- or mesoscopic structures leads to memory effects at the macroscopic level. Future work will have to clarify the range of these memory effects and if the Markovianity approaches information flow in the limit of an infinite history.

²See [6], Chapter 7, for all details.

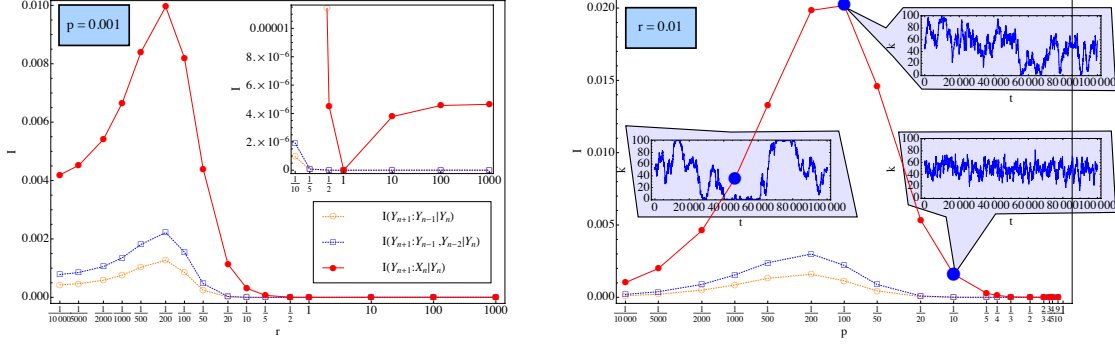


Figure 4: Information flow and Markovianity for the two-community voter model. L.h.s.: Closure measures as a function of the ratio r between strong and weak ties. R.h.s.: Closure measures as a function of the contrarian rate p with which agent do not imitate their interlocutor.

4 Multi levels approach and mean-field methods in neuroscience

In this section we investigate examples of neuronal modelling where the general strategy described in section 1 is worth applying. Typically, a neuronal system is composed of several populations of thousands of neurons, connected in a complex way. So, it is tempting to use the mean-field techniques developed in physics, consisting of replacing a population of particles by some quantity (density, field, tensor, order parameter) summarizing the relevant properties of this population, to understand the meso- or macro-scopic dynamics. That is, one wants precisely to implement the shift in the levels of description described by fig. 1.

As we shall see, it is easy to write down phenomenological equations that perfectly fit in this program and, additionally, meet success when applied to the real brain. However, when one wants to obtain these mesoscopic equations from the microscopic dynamics, some unexpected questions arise, leading to situations where Fig. 1 or at least its Markovian version Fig. 3 breaks down. Such an examples is fully developed here.

4.1 The model

In this section we consider a specific class of neural networks model, based on firing rates, introduced by Amari in 1972 and Wilson-Cowan the same year [1, 40]. The equation of evolution reads:

$$\frac{dV_i}{dt} = -\frac{V_i}{\tau_i} + \sum_{j=1}^N W_{ij} f_j(V_j(t)) + I_i(t) + \sigma \xi_i(t); \quad i = 1 \dots N, \quad (10)$$

where $V_i(t)$ is the membrane potential of neuron i at time t , τ_i is the leak rate time constant of neuron i . W_{ij} denotes the synaptic interaction weight from j (pre-synaptic neuron) to i (post-synaptic neuron). The W_{ij} s do not evolve in time. We have $W_{ij} = 0$ when j and i are not connected. f_j is a function characterizing the response curve of neuron j , i.e. how does the firing rate of neuron j depends on its membrane potential. We take here a sigmoid, e.g. $f_j(x) = \frac{1 + \operatorname{erf}(\frac{g_j x}{\sqrt{2}})}{2}$. The parameter g_j ("gain") controls the nonlinearity of

the sigmoid. $I_i(t)$ represents an external stimulus imposed upon neuron i . $\xi_i(t)$ is a white noise, whose amplitude is controlled by σ . Thus, (10) is a non linear stochastic equation (written in physicists form, for simplicity).

Note that eq. (10) is already a mean-field equation as the spike activity has been replaced by the firing rate function $f_j(x)$.

A variant of eq. (10) is a multi-population model, where neurons are divided in P populations $a = 1 \dots P$, with N_a neurons in population a , $N = \sum_{a=1}^P N_a$ [21]. By "population", we mean that neurons can be grouped into subsets having the same characteristics. In the present model, those characteristics are the membrane time constant, the firing rate function, which depends therefore only on the population (e.g. the gain $g_i = g_a$ on population a). We have thus:

$$\frac{dV_i}{dt} = -\frac{V_i}{\tau_a} + \sum_{b=1}^P \sum_{j=1}^{N_b} W_{ij} f_b(V_j(t)) + I_a(t) + \sigma \xi_i(t); \quad i \in a, a = 1 \dots P. \quad (11)$$

4.2 The naive mean-field equations

We are interested in the mean evolution of membrane potential averaged over neuronal population, in the large number of neurons limit, $V_a(t) = \lim_{N_a \rightarrow \infty} \frac{1}{N_a} \sum_{i=1}^{N_a} V_i(t)$, assuming this limit exists. To make things simpler in the beginning, assume for a while that W_{ij} only depends on the presynaptic (b) and post synaptic (a) population, i.e. $W_{ij} = \frac{\bar{W}_{ab}}{N_b}$, $i \in a, j \in b$, where the scaling factor $\frac{1}{N_b}$ ensures that the sum $\sum_{j=1}^{N_b} W_{ij} f_b(V_j(t))$ does not diverge as $N_b \rightarrow +\infty$. We obtain:

$$\frac{dV_a}{dt} = -\frac{V_a}{\tau_a} + \sum_{b=1}^P \bar{W}_{ab} \phi_b(t) + I_a(t); a = 1 \dots P, \quad (12)$$

with:

$$\phi_b(t) = \lim_{N_b \rightarrow +\infty} \frac{1}{N_b} \sum_{j=1}^{N_b} f_b(V_j(t)), \quad (13)$$

and where we have used $\lim_{N_a \rightarrow +\infty} \frac{1}{N_a} \sum_{i=1}^{N_a} \xi_i(t) = 0$ (almost-surely).

Eq. (12) almost retains the structure of eq. (10), at the level of populations (mesoscopic level). However, the big difference is obviously the function $\phi_b(t)$ averaging the non linear influence of population b on population a activity. In order to have exactly the same structure we would like to write something like $\phi_b(t) = f_b(V_b(t))$ giving what we call the "naive-mean field equations":

$$\frac{dV_a}{dt} = -\frac{V_a}{\tau_a} + \sum_{b=1}^P \bar{W}_{ab} f_b(V_b(t)) + I_a(t); \quad a = 1 \dots P. \quad (14)$$

In this case, the mean-field equation, at the level of average membrane potential population has the same form as the initial equation, at the microscopic level of membrane potentials of neurons. This is a simple example that fits with fig. 1 and 3 (in the continuous time case).

4.3 The commutation assumption

Inspected from the mathematical point of view this corresponds to assuming that:

$$\lim_{N_b \rightarrow +\infty} \frac{1}{N_b} \sum_{j=1}^{N_b} f_b(V_j(t)) = f_b \left(\lim_{N_b \rightarrow +\infty} \frac{1}{N_b} \sum_{j=1}^{N_b} V_j(t) \right), \quad (15)$$

a commutation property which is wrong in general, as soon as f_b is non linear. Even when V_j s are random i.i.d. variables does this assumption fail. A trivial case where it holds however is when all $V_j(t)$ have the same value.

However, many mean field equations dealing with average activity at the level of populations use the commutation of sigmoidal nonlinearity and membrane potential average. Examples are Jansen-Ritt equations for cortical columns [27, 21] [22]. Although these equations are posed ad hoc without mathematical justification, assuming that they hold at the mesoscopic level and, at the same time, that eq. (10) holds true at the neuronal microscopic level somewhat implies the assumption of commutation.

As (15) holds at least when all $V_j(t)$ have the same value, trivially equal to the mean value, it is reasonable to guess that (15) is broken down by fluctuations about the mean. How these fluctuations modify the evolution equation, and giving one example where the correct form of mean field dynamics at the mesoscopic level is known, is the topic of this section.

4.4 Random synaptic weights

We are going to obtain the correct mean field equations in the following case. In section 4.2 we have considered that W_{ij} is depending only on the population of pre- and post-synaptic neurons, with a value $\frac{\bar{W}_{ab}}{N_b}$. Here, we extend this situation considering W_{ij} as *independent* Gaussian random variables whose law depends only on a and b , where W_{ij} has mean $\frac{\bar{W}_{ab}}{N_b}$ and variance $\frac{\sigma_{ab}^2}{N_b}$, for $i \in a, j \in b$. Thus, we keep the idea of having an average connectivity strength $\frac{\bar{W}_{ab}}{N_b}$ between population b and a , but we now allow fluctuations about the mean and we suppose these fluctuations are uncorrelated. The scaling of the variance ensures that the term $\sum_{b=1}^P \sum_{j=1}^{N_b} W_{ij} f_b(V_j(t))$ in eq. (11) has finite and non vanishing fluctuations in the limit $N_b \rightarrow +\infty$. A scaling $\frac{1}{N_b^2}$ leads actually to naive mean-field equations since in this case all V_i s follow the same trajectory [1, 24].

The goal now is to obtain a description of the average behaviour of (11), in the limit $N_b \rightarrow +\infty, b = 1 \dots P$ (thermodynamic limit), where the average is taken both on white noise and synaptic weights distribution (quenched average). We note $[\]$ the expectation w.r.t. weights and $\langle \ \rangle$ the expectation w.r.t. noise.

Taking this average is somewhat the easiest thing to do, in a probabilistic sense (although already quite complex). Indeed, considering the behaviour of averages when taking the infinite size limit corresponds to weak-convergence. Stronger results would deal with almost-sure convergence, namely the typical (on a full measure set) behaviour of a given network in the thermodynamic limit. Such results require however large deviations theory and will not be addressed here. See [31, 20].

This case has been studied, for the first time, by Sompolinsky and co-workers in the model (10), without noise, without external current, with $f(x) = \tanh(gx)$ which introduces a convenient symmetry $x \rightarrow -x$ in the problem (0 is always a fixed point). Exten-

sions to discrete time model with broken symmetry $x \rightarrow -x$ has been done in [17, 15, 16] whereas a multi populations model has been considered in [21].

4.5 Methods to obtain mean-field equations

The exact mean-field equations can be derived in 3 ways:

- (i) The local chaos hypothesis introduced by Amari in 1972 [1] for the continuous time dynamics (10) and used by Cessac and coworkers for a discrete version [17, 15, 16];
- (ii) Using the functional generating approach developed for spin-glasses and used, for the first time, by Sompolinsky and coworkers [36], for the continuous time dynamics (10), and Molgedey et al for the model (10) [30];
- (iii) Using the large deviations technique introduced by Guionnet and Ben Arous for spin-glasses [11] and used by Moynot and Samuelides [31] for a discrete version of (10).

These 3 methods lead to the same mean-field equations. The advantage of (i) is to be straightforward, although relying on a quite questionable hypothesis (explained below). The method (ii) belongs to the standard toolbox of physics and is more natural to physicists. To our best knowledge it is the only method up to now³ allowing to study which mean-field solutions are actually observed in the limit $N \rightarrow +\infty$. In its most recent version it requires a sophisticated formalism (supersymmetry [14]) and still relies on questionable assumptions: typically the ad hoc cancellation of an auxiliary field used in the computation. The advantage of (iii) is to be rigorous and to extend to the correlated case [20]. The price to pay is a rather huge mathematical background.

In order to rapidly present the mean-field equations in the uncorrelated case, we shall focus here on method (i).

4.6 Mean-field equations from local chaos hypothesis

The local chaos hypothesis assumes that, in the thermodynamic limit, neurons become independent from each others and from the W_{ij} s. Actually, a weaker property has been proved in [24, 31], the "propagation of chaos": for any subset of k neurons, with k finite, those neurons become independent in the thermodynamic limit. Denote:

$$U_{ib}(t) = \sum_{j=1}^{N_b} W_{ij} f_b(V_j(t)); \quad i \in a, \quad (16)$$

the sum of "influences" received by neuron $i \in a$, coming from the synaptic population b . From Central Limit Theorem the first consequence of local chaos hypothesis, is that, in the limit $N \rightarrow +\infty$, $U_{ib}(t)$ converges in law to a Gaussian process U_{ab} whose law depends only on population index a and b . Moreover, local chaos hypothesis allows to compute easily the mean and covariance of this process.

One ends up with the following conclusions.

³In principle, large deviations should also allow this study though this has not been done yet.

1. In the thermodynamic limit all neurons in population a have a membrane potential with the same probability distribution. We denote this potential by V_a . Then, eq. (11) becomes, in the thermodynamic limit:

$$\frac{dV_a}{dt} = -\frac{V_a}{\tau_a} + \sum_{b=1}^P U_{ab}(t) + I_a(t) + \sigma \xi_a(t); \quad i \in a, a = 1 \dots P. \quad (17)$$

where $\xi_a \sim \xi_i$.

2. U_{ab} is a Gaussian process with mean and covariance given by:

$$[\langle U_{ab}(t) \rangle] = \bar{W}_{ab} [\langle f_b(V_b(t)) \rangle]; \quad (18)$$

$$\text{Cov} [U_{ab}(t) U_{cd}(s)] = \sigma_{ab}^2 \delta_{ac} \delta_{bd} [\langle f_b(V_b(t)) f_b(V_b(s)) \rangle]. \quad (19)$$

3. V_a is a Gaussian process with mean and covariance given by:

$$[\langle V_a(t) \rangle] = \sum_{b=1}^P \bar{W}_{ab} \int_{t_0}^t [\langle f_b(V_b(t)) \rangle] e^{-\frac{(t-s)}{\tau_a}} ds + \int_{t_0}^t I_a(s) e^{-\frac{(t-s)}{\tau_a}} ds \quad (20)$$

$$\text{Cov} [V_a(t), V_c(t')] = \quad (21)$$

$$\delta_{ac} \sum_{b=1}^P \sigma_{ab}^2 \int_{t_0}^t \int_{t_0}^{t'} [\langle f_b(V_b(t)) f_b(V_b(s)) \rangle] e^{-\frac{(t+t'-s-s')}{\tau_a}} ds ds' + \frac{\sigma^2 \tau_a}{2} \left[1 - e^{-\frac{2(t-t_0)}{\tau_a}} \right],$$

with $t \leq t'$.

These equations constitute a closed set of self-consistent equations, called mean-field equations.

4.7 From exact mean-field equations to naive ones

$V_a(t)$ being Gaussian it is easy to obtain the evolution equation of $[\langle V_a(t) \rangle]$. We have:

$$\frac{d[\langle V_a \rangle]}{dt} = -\frac{[\langle V_a \rangle]}{\tau_a} + \sum_{b=1}^P \bar{W}_{ab} \int_{-\infty}^{+\infty} f_b \left(h \sqrt{\sigma_b(t)} h + [\langle V_b(t) \rangle] \right) Dh + I_a(t), \quad (22)$$

with $Dh = \frac{1}{\sqrt{2\pi}} e^{-\frac{h^2}{2}}$ and where:

$$\begin{aligned} \sigma_b(t) = & \sum_{b'=1}^P \sigma_{bb'}^2 \int_{t_0}^t \int_{t_0}^t \frac{1}{2\pi \det C_{b'}(s, s')} \left[\int_{-\infty}^{+\infty} \int_{-\infty}^{+\infty} f_{b'}(u) f_{b'}(v) e^{-\frac{1}{2} X^\dagger C_{b'}^{-1}(s, s') X} dX \right] e^{-\frac{(2t-s-s')}{\tau_b}} ds ds' \\ & + \frac{\sigma^2 \tau_b}{2} \left[1 - e^{-\frac{2(t-t_0)}{\tau_b}} \right]. \end{aligned} \quad (23)$$

Here,

$$C_{b'}(s, s') = \begin{pmatrix} \text{Cov} [V_{b'}(s), V_{b'}(s)] & \text{Cov} [V_{b'}(s), V_{b'}(s')] \\ \text{Cov} [V_{b'}(s'), V_{b'}(s)] & \text{Cov} [V_{b'}(s'), V_{b'}(s')] \end{pmatrix}, \quad (24)$$

with:

$$\begin{aligned} \text{Cov} [V_b(t), V_b(t')] = & \sum_{b'=1}^P \sigma_{bb'}^2 \int_{t_0}^t \int_{t_0}^{t'} \frac{1}{2\pi \det C_{b'}(s, s')} \left[\int_{-\infty}^{+\infty} \int_{-\infty}^{+\infty} f_{b'}(u) f_{b'}(v) e^{-\frac{1}{2} X^\dagger C_{b'}^{-1}(s, s') X} dX \right] e^{-\frac{(t+t'-s-s')}{\tau_b}} ds ds' \\ & + \frac{\sigma^2 \tau_b}{2} \left[1 - e^{-\frac{2(t-t_0)}{\tau_b}} \right], \end{aligned} \quad (25)$$

whereas X is the vector $\begin{pmatrix} u \\ v \end{pmatrix}$ and † denotes the transpose.

Inspecting equations (22) one sees that the evolution of the average is constrained by the time integrations of fluctuations, and those fluctuations are themselves constrained by a set of self-consistent equations (24), (25), where the covariance $\text{Cov} [V_b(t), V_b(t')]$ *integrates the whole history of correlations from the initial time t_0* . As a consequence, this evolution is non-Markovian as it integrates the whole history. In this sense, although eq. (17) looks like a dynamical system equations, it is not: the term $\sigma_b(t)$ introduces a whole history dependence of the trajectories.

Clearly, although eq. (22) looks very similar to (14) they are deeply different. Note, however that if fluctuations vanish ($\sigma_b(t) = 0$) both equations are identical.

4.8 Mean-Field solutions

Solving those equations is a formidable task. To our best knowledge it has been achieved in only one case, for one population, $f(x) = \tanh(gx)$, $I_a = 0$, no noise, by Sompolinsky et al, [36]. Assuming stationarity, they were able to show the quantity $\Delta(\tau) = [\langle V(t)V(t') \rangle]$, $\tau = t' - t$ obeys the Newton equation:

$$\frac{d^2 \Delta}{d\tau^2} = -\frac{\partial \mathcal{V}}{\partial \Delta}$$

for some potential \mathcal{V} that can be explicitly written. From this it is easy to draw the phase portrait and infer the time evolution of Δ . From this analysis these authors were able to show the existence of several dynamical regimes, from stable fixed point, to periodic solutions, to chaos. Moreover, the dynamic mean field method they used, based on generating functional, allowed to show that periodic solutions are in fact not observable in the thermodynamic limit. Analysis of the finite dimensional system confirms this result: there is transition to chaos by quasi-periodicity when increasing the parameter g where the intermediate phase (periodic orbits and T^2 torus) occurs on a g range that vanishes as $N \rightarrow +\infty$ [17, 16].

4.9 Discussion

In this section we have given an example where mean-field equations at the mesoscopic level can be obtained from microscopic dynamics, by performing a suitable averaging. However, the structure of mean-field equations is in general quite different from the microscopic ones. Going to the mean-field, one replace N equations by eq. (17), (24), (20), but the price to pay is the inheritance of a non Markovian structure, extremely hard to integrate even numerically. Here, averaging over the synaptic weights fluctuations produces therefore

a mean-field dynamics rather difficult to interpret, requiring new tools and concepts, in the spirit of those developed for spin-glasses in the eighties, although with a different, non relaxational dynamics [37]. Additionally, introducing weights correlations, which are expected as soon as one e.g. introduces synaptic plasticity complexifies even more the picture [19, 32, 20].

In the context of this paper and of the general scheme of fig. 1 and 3, one clearly sees that fluctuations induced by synaptic weights inhomogeneity breaks down the Markov property of the initial equations. At first glance, it looks to be generated by the somewhat artificial procedure of averaging over synaptic weights and noise. This is partly true. However, the problem is deeper. Indeed, as we said above, the averaging corresponds, in a probabilistic context, to a weak form of convergence as the number of neurons tends to infinity. A stronger type of convergence (e.g. almost-sure, i.e. for a measure one set of synaptic weights and noise trajectory selection) would be preferable. Now, if almost sure convergence holds, the solution has to converge to the weak solution, the one we found here. In this case, we obtain, that for almost-every realisation of networks and noise, the mean-field solution actually also breaks down the Markovianity.

As we remarked in subsection 4.3, the naive mean-field equations are exact when when all $V_j(t)$ have the same value, a rather exceptional situation. This can however be considered as a good approximation to the case when fluctuations (controlled by the term σ_b in (22)) are small. In any other cases, the relevant equations are the non Markovian dynamic mean field equations, which produce quite a non trivial dynamics.

As a final remark, note however that the equations for covariance includes an exponential decay with time, so that a Markovian approximation with time cut-off can easily be proposed.

5 Renormalization group coarse-graining and effective theories

In the other sections of the paper, we have considered the dynamical models, in which the relations between spatial and temporal components are specified explicitly – by the equations of motion. In the present section, we change our point of view and work with the generalized *scaling degrees of freedom* – in which time and space are not explicitly distinguished against each other – instead of the physical degrees of freedom discussed in the other sections. The scaling degrees of freedom are related to the physical degrees of freedom of the original model by means of the Renormalization Group (RG) transformations (which we discuss below) and thus enjoy a renormalization group structure, a kind of symmetry that might facilitate their investigation.

The results obtained from the RG analysis are considered as a statistical steady-state limit, the most likely behavior to be observed in the physical system, without any regard to neither a particular way the system can evolve towards the steady-state, nor the duration of transition to it. The (infinitely) long-time (infinitely) large-scale asymptotes of the correlation functions derived from the RG study differ from their physical analogs by the amplitude factors (normalizations) and thus can be efficiently used for the analysis of systems for which a scale-free behavior is observed.

The renormalization group (RG) was initially devised in elementary particle physics, but nowadays its applications extend to solid-state physics, fluid mechanics, and cosmology [41, 42, 29, 38]. The main idea ("blocking") in RG theory is a way to define the components of the system at large distances as aggregates of components at shorter distances. The

system at one scale is generally seen to consist of self-similar copies of itself when viewed at a smaller scale. The parameters of the theory typically describe the interactions of the components that may relate to atoms, elementary particles, atomic spins, but also may appear to be composed of more of the self-same components as one goes to shorter distances. As the strength of forces exerted in an interaction between the individual components – coupling – changes with scale, the so-called renormalization flow (or RG flow) of parameters in the theory is induced. The running of coupling strength with scale stops (at a fixed point attained for particular values of the coupling parameters) when the system is scale-invariant. The possible macroscopic states of the system, at a very large scale, are given by the set of fixed points of the RG flow.

The idea of RG is therefore to build an *effective theory* for the long-distance degrees of freedom that is achieved by summing out all short distance degrees of freedom within macroscopic components of the system. If the system is known to be scale-invariant, the universal quantities we are interested in do not matter crucially on the short distances, at least it should be possible to devise reasonable approximations that preserve the scale invariance property at long distance.

Metaphorically speaking, the idea of RG is akin to the principle of a kaleidoscope that multiply reflects loose objects such as bits of glass generating an infinite regular grid of self-same duplicate images. The rotation of the kaleidoscope tube plays the role of a changing scale in the RG theory, and at some characteristic angles (at the fixed points of the RG transformation) the kaleidoscope mirrors show up the tumbling of the glass bits as the infinite beautiful symmetrical patterns created by the reflections that fills the entire field.

5.1 Block transformation in one dimension

Let us start by a simple and illuminating example of Wilson’s RG method applied to the one-dimensional Ising model with nearest neighbor interactions [10] – the chain of spins (Fig. 5). The Hamiltonian function for the one-dimensional Ising model is

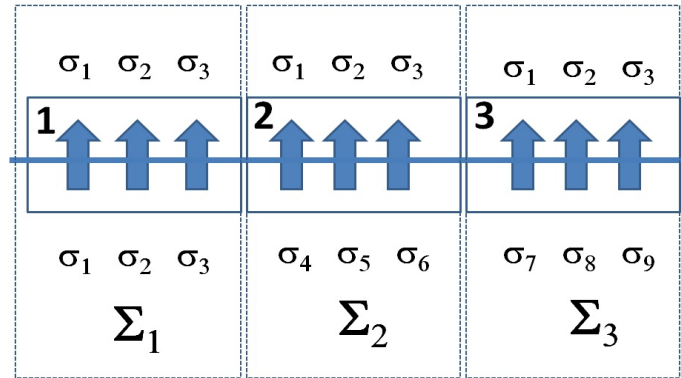


Figure 5: The one-dimension spin lattice.

$$H_0 = -K \sum_{i=1}^N \sigma_i \sigma_{i+1} \quad (26)$$

where $K = \frac{J}{\beta}$ is the coupling constant and $\sigma_i = \pm 1$ is the spin, and the partition function becomes

$$Q = \text{Tr}_\sigma e^{-H_0}. \quad (27)$$

Rather than summing over all the spins at once, we will implement the renormalization group philosophy of summing over the modes associated with the short length scales first. Let us consider a simple block spin transformation as illustrated in Fig. 5. The figure shows the one-dimension spin lattice numbered in two different ways - one a straight numbering and one using blocks of three spins, with spins in each block numbered 1-3. The block spin transformation to be employed here is that the spin of a block will be determined by the value of the spin in the center of the block. Thus, for block 1, it is the value of σ_2 , for block 2, it is the value of σ_5 , etc.

The blocking transformation function, for this case is

$$T(\Sigma; \sigma_1, \sigma_2, \sigma_3) = \delta_{\Sigma, \sigma_2}, \quad (28)$$

where $\delta(x)$ is the Dirac delta function. The new block-lattice will look like the chain of big boxes shown in Fig. 5 with $\Sigma_1 = \sigma_2$, $\Sigma_2 = \sigma_5$, etc. The transformed, block Hamiltonian is computed from

$$\begin{aligned} e^{-cH(\Sigma)} &= \sum_{\sigma_1} \dots \sum_{\sigma_N} (\delta_{\Sigma_1, \sigma_2} \delta_{\Sigma_2, \sigma_5} \dots) e^{K\sigma_1\sigma_2} e^{K\sigma_2\sigma_3} e^{K\sigma_3\sigma_4} \dots \\ &= \sum_{\sigma_1} \sum_{\sigma_3} \sum_{\sigma_4} \dots e^{K\sigma_1\Sigma_1} e^{K\Sigma_1\sigma_3} e^{K\sigma_3\sigma_4} e^{K\sigma_4\Sigma_2} \dots \end{aligned} \quad (29)$$

The idea of RG is then to find the new coupling constant K' such that when the sum over σ_3 and σ_4 are performed, the new interaction between the block spins, Σ_1 and Σ_2 , is of the form $\exp(K'\Sigma_1\Sigma_2)$, which preserves the functional form of the old Hamiltonian.

The sum over σ_3 and σ_4 ,

$$\sum_{\sigma_3} \sum_{\sigma_4} e^{K\Sigma_1\sigma_3} e^{K\sigma_3\sigma_4} e^{K\sigma_4\Sigma_2}$$

is easy to calculate if we note that $\sigma_3\sigma_4 = \pm 1$ and that $e^{\pm\theta} = \cosh\theta \pm \sinh\theta = \cosh\theta [1 \pm \tanh\theta]$. Then

$$e^{K\sigma_3\sigma_4} = \cosh K [1 + \sigma_3\sigma_4 \tanh K],$$

and we search for such K' that

$$\sum_{\sigma_3} \sum_{\sigma_4} e^{K\Sigma_1\sigma_3} e^{K\sigma_3\sigma_4} e^{K\sigma_4\Sigma_2} = 2 \cosh^3 K [1 + \Sigma_1\Sigma_2 \tanh^3 K]$$

preserves the old functional form

$$\equiv \cosh K' [1 + \Sigma_1\Sigma_2 \tanh^3 K'].$$

The latter requirement is nothing else but the RG equation, determining the RG flow for this particular block spin transformation. The solution of such a RG equation is obviously

$$K' = \text{arctanh} [\tanh^3 K]. \quad (30)$$

With this identification of K' , the new, renormalized Hamiltonian can be shown to be

$$H' = N'g(K) - K' \sum_{i=1}^{N'} \Sigma_i \Sigma_{i+1} \quad (31)$$

where N' is the new, reduced number of spin blocks, and the spin-independent function $g(K)$, is given by

$$g(K) = -\frac{1}{3} \ln \left[\frac{\cosh^3 K}{\cosh K'} \right] - \frac{2}{3} \ln 2. \quad (32)$$

Apart from the additional term, the new Hamiltonian (31) is exactly of the same functional form as the original Hamiltonian (26) but with a different set of spin variables and a different coupling constant. The transformation can now be applied to the new Hamiltonian, yielding the same relation between the new and old coupling constants. This is equivalent to iterating the RG equation. However, in an ordered phase – the specific macrostate – the transformed lattice would be exactly the same as the old lattice, and hence the same coupling constant and Hamiltonian would result. Such a point (if it exists) is nothing else but a fixed point of the RG equation and is given in the above model by the condition

$$\tanh K = \tanh^3 K, \quad (33)$$

with two obvious solutions

$$\tanh K = 0, \quad \text{and} \quad \tanh K = 1, \quad (34)$$

which are the fixed points of the RG equation.

The iteration of the RG equation,

$$\tanh K_{n+1} = \tanh^3 K_n, \quad (35)$$

produces an RG flow through coupling constant space. The fixed point at $K = 1$ is an unstable fixed point because any perturbation away from it, if iterated through (35), flows away from this point to the another, stable fixed point $K = 0$. As the stable fixed point is approached, the coupling constant gets smaller and smaller until, at the fixed point, it is 0.

Since $K \sim 1/T$, the inverse temperature, $K \rightarrow 0$ corresponds to high temperature, and $K \rightarrow 1$ corresponds to low temperature. The absence of a fixed point for any finite, nonzero value of temperature tells us that there can be no ordered phase and, hence, a phase transition in one dimension. If there were a critical point at some temperature T_c , then, at that point, long range order would set in, and there would be a fixed point of the RG equation at $K_c \sim 1/T_c$.

5.2 Towards effective theories through perturbations

The idea behind perturbation theory is to find an approximate solution to a problem, by starting from the exact solution of a related, simpler, linear problem. Perturbation theory is applicable if the problem at hand cannot be solved exactly, but can be formulated by adding a “small”, perturbation term to the description of the exactly solvable problem. If we consider an exactly soluble model – either the Gaussian or the mean field model – and add the term(s) present in the model under study, which are not taken into account in the exactly soluble model, we obtain an expression for the desired solution in terms of

a formal power series in the “small” parameter – known as a perturbation series – that quantifies the deviation from the exactly solvable problem [41, 42, 38].

For instance, let us consider the well-known ϕ^4 model which belongs to the same universality class as the Ising model. The partition function for the ϕ^4 model is given by

$$Z(A) = \int \mathcal{D}\phi e^{-H(\phi) + \int A\phi} \quad (36)$$

where A is the external source field, the symbol $\int \mathcal{D}\phi$ denotes the functional integration over all possible configurations of the field ϕ , and the Hamiltonian function takes the form

$$H(\phi) = \int d^d x \left(\frac{1}{2} (\nabla\phi)^2 + \frac{1}{2} r_0 \phi^2 + \frac{1}{4!} g_0 \phi^4 \right). \quad (37)$$

The validity of such an expansion is predicated upon the actual physics of our system being close to that of a free field (Gaussian) system. In this case, we may calculate observables by summing the leading terms in the expansion. In particular, it is possible to take the Gaussian model as a reference,

$$Z_0(A) = \int \mathcal{D}\phi e^{-H_0(\phi) + \int A\phi}, \quad (38)$$

where

$$H_0(\phi) = \int d^d x \left(\frac{1}{2} (\nabla\phi)^2 + \frac{1}{2} r_0 \phi^2 \right), \quad (39)$$

and develop Z as a series in g_0 around Z_0 :

$$Z = \int \mathcal{D}\phi \left(1 - \frac{g_0}{4!} \int_{x_1} \phi^4(x_1) + \frac{1}{2} \left(\frac{g_0}{4!} \right)^2 \int_{x_1, x_2} \phi^4(x_1) \phi^4(x_2) + \dots \right) e^{-H_0 + \int A\phi}. \quad (40)$$

This expansion leads to the series of Feynman diagrams for the various correlation functions $\langle \phi(x_i) \dots \phi(x_j) \rangle$ of the distant arguments x_i, x_j . Feynman diagrams represent the summation over probability amplitudes corresponding to all possible exchanges of virtual particles compatible with a given process at a given order.

The problem with this approach is that the “fluctuations” induced by the ϕ^4 term around the Gaussian model are large. In the perturbation expansion the degrees of freedom can be cast in terms of the Fourier modes – in space and in time simultaneously – of a given field. Then the “fluctuations” induced by the ϕ^4 lead to integrals – corresponding to the loops in the Feynman diagrams – that are supposed to be calculated with the cut-off at the upper bound Λ , an *ultraviolet* regulator related to high-momentum (large-wavenumber) modes in the physical space. If Λ was sent to infinity, the integrals would be generically divergent. This means that for Λ finite but large, the integrals are large and depend crucially on the value of Λ .

The RG transformation proceeds by integrating out a certain set of high-momentum (large-wavenumber) modes that allows to re-parameterize (by coarse-graining) the perturbation expansion in such a way that the sensitive dependence on Λ has been eliminated. Since large wave numbers are related to short-length scales, the momentum-space RG results in an essentially similar coarse-graining effect as with real-space RG. Therefore, the renormalization group allows to partially resume the perturbation expansions and thus to compute universal behaviors [41, 42, 38].

The way fluctuations are summed over in perturbation theory is not appropriate since fluctuations of all wavelengths are treated on the same footing in Feynman diagrams. In

order to organize the summation over fluctuations in a better way, we can build an effective theory for the long-distance degrees of freedom. This is achieved by integrating out the short distance ones. Since, at least for universal quantities, these short distance quantities do not matter crucially, it should be possible to devise approximations that preserve the physics at long distance.

Schematically, to implement the RG method, we divide the Fourier space $\phi(p)$ into two pieces: $\phi_>(p)$ that involves the *rapid* modes $p \in [\Lambda/s, \Lambda]$ of $\phi(p)$ and $\phi_<(p)$ that involves the *slow* modes $p \in [0, \Lambda/s]$. The use of words 'rapid' and 'slow' in the present context should not puzzle the reader as we work with the Fourier modes, so that the field ϕ is defined on the set of plain waves of different wave numbers. Then, the partition function can be written down as

$$Z = \int \mathcal{D}\phi_< \int \mathcal{D}\phi_> e^{-H(\phi_<, \phi_>, \Lambda, K)}, \quad (41)$$

where K represents all possible coupling constants compatible with the symmetries of the system. The integration of the rapid modes consists in integrating out the $\phi_>$ field. In this integration, all the couplings K start to grow but the functional form of the Hamiltonian H remains unchanged. Let us define the series of coupling constants, each associated with a given scale s ,

$$\Lambda \mapsto K, \quad \frac{\Lambda}{s} \mapsto K', \quad \frac{\Lambda}{s^2} \mapsto K'', \quad \text{etc.}$$

Namely, we use the bare cut-off parameter Λ in the original partition function, and the rescaled cut-off parameter Λ/s^k in the partition function with the coupling constant $K^{(k)}$ such that

$$e^{-H(\phi_<, K', \Lambda/s)} = \int \mathcal{D}\phi_> e^{-H(\phi_<, \phi_>, K, \Lambda)}, \quad \text{etc.}$$

The flow of coupling constants $K \rightarrow K' \rightarrow K'' \rightarrow \dots$ is sufficient to obtain much information on the physics of the system under study. It is remarkable that to different K s on the same RG trajectory correspond systems that are albeit microscopically different but that nevertheless can lead to the same long-distance behavior, since they all have the same partition function and provided they belong to the same basin of attraction K^* , the fixed point characterizing the same universality class of the long-distance behavior.

Asymptotic solutions for the nonlinear models of critical dynamics can also be obtained in the form of a perturbation theory [39]. In many cases, the Feynman diagram series of perturbation theory can be studied by means of the renormalization group method – with the use of the simple diffusion process as an exactly solvable reference model – that allows calculating the critical exponents related to the phase transitions in renormalizable models. Dynamical models admit two scales—spatial and temporal—and, consequently, their partition functions are invariant with respect to two independent scale transformations (in space and in time). Hence, all fields and parameters of the theory (Q) have two independent *canonical* dimensions, the momentum dimension d^k , and the frequency dimension d^ω , $d[Q] = d^k[Q] + 2d^\omega[Q]$, expressing the fact that the first time derivative corresponds to the second order spatial derivative in the diffusion process. In the renormalization of dynamical models the total dimension $d[Q]$ plays the same role as the ordinary (momentum) dimension in static problems discussed above. These canonical dimensions by no means coincide with the *critical* dimensions of the same quantities,

$$\Delta[Q] = d^k[Q] + \Delta[\omega]d^\omega[Q] + \gamma_Q, \quad (42)$$

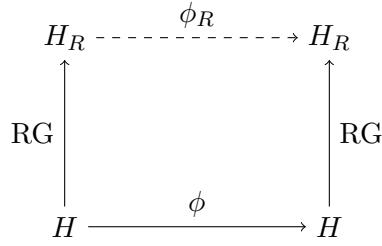


Figure 6: Schematic view of the renormalization procedure as a multi-level system.

where Q is any quantity of the theory, $d^k[Q]$ and $d^\omega[Q]$ are the relevant momentum and frequency canonical dimensions, $\Delta[\omega] = 2 + \gamma_\omega$ is the critical dimension of frequency, γ_Q and γ_ω are the *anomalous* dimensions of Q and ω consequently. The anomalous dimensions γ can be calculated in the form of ε -expansions.

In contrast to the approaches discussed in the other sections of the paper, the method of RG operates with the scaling degrees of freedom—in which time and space are not explicitly distinguished against each other. The use of RG techniques can facilitate the long-time large-scale asymptotic analysis of the physical system as it concerns the scaling degrees of freedom enjoying the group structure, in contrast to the physical degrees of freedom of the original problem. A semi-group of RG transformations that maps a Hamiltonian into another Hamiltonian by the elimination of short-range degrees of freedom (micro - variables), with respect to which the partition function of the system remains invariant, provides a remarkable example of a level transformation in multi-level systems. Indeed, while the old Hamiltonian can be viewed as corresponding the original system X described by "micro-variables" in the diagram shown in Figure 1, the new Hamiltonian that does not contain the short-range degrees of freedom describes the system using a different, "renormalized" set of variables (macro-variables) and corresponds to another, "coarse-grained" state space Y . The function π in the diagram representing the passage from the X - set of variables to the Y -set is nothing else but the Renormalization Group transformation.

In Figure 2, we have schematically shown the relation between the non-renormalized Hamiltonian (H) and the coarse-grained, renormalized Hamiltonian (H_R) by means of the Renormalization Group transformation RG. The original dynamics (ϕ) is replaced by the renormalized dynamics (ϕ_R) in the renormalized theory.

6 Quantum decoherence as a multi-level system

The notion of environmental decoherence has been widely discussed and accepted as the mechanism by which classicality emerges in a quantum world. Decoherence explains why we tend not to observe quantum behavior in everyday macroscopic objects. For example, one of the most revolutionary elements introduced into physical theory by quantum mechanics is the superposition principle. If $|1\rangle$ and $|2\rangle$ are two states, then quantum mechanics tells us that any linear combination $\alpha|1\rangle + \beta|2\rangle$ also corresponds to a possible state. Whereas such superposition of states have been experimentally extensively verified for microscopic systems, it is apparently not the case of the everyday world – a Schrödinger cat that is a superposition of being alive and dead does not bear much resemblance to reality as we perceive it. Why does the world appear classical to us, in spite of its supposed

underlying quantum nature? Quantum decoherence also explains why we do see classical fields emerge from the properties of the interaction between matter and radiation for large amounts of matter.

Quantum decoherence can be viewed as the loss of information from a system into the environment (often modeled as a heat bath), since every system is loosely coupled with the energetic state of its surroundings. Viewed in isolation, the system's dynamics are non-unitary (although the combined system plus environment evolves in a unitary fashion). Thus the dynamics of the system alone are irreversible. As with any coupling, entanglements are generated between the system and environment. These have the effect of sharing quantum information with, or transferring it to, the surroundings. Quantum decoherence represents an extremely fast process for macroscopic objects, since these are interacting with many microscopic objects, with an enormous number of degrees of freedom, in their natural environment.

As we show in this section, it is remarkable that quantum decoherence provides an example of a multi-level system, in which the time evolution of observables is reduced to a completely positive dynamical map under conditional expectation and then, can be replaced by the effective dynamics, as time tends to infinity. In this section, we follow our joint presentation with Mario Hellmich on decoherence in infinite quantum systems [12].

6.1 Setting the stage

In the standard interpretation of quantum mechanics, a measurable operator in a Hilbert space – an observable corresponding to a physical quantity – has a definite value if and only if the system is in an eigenstate of the observable. If the system is in a superposition of such eigenstates, according to the orthodox interpretation, it is meaningless to speak of the state of the system as having any definite value of the observable at all. In a typical laboratory experiment involving some physical system, we can identify two subsequent phases: a preparation which is followed by a measurement.

In the ideal measurement scheme a microscopic system \mathcal{S} , represented by basis vectors $\{|s_n\rangle\}$ in a Hilbert space $\mathcal{H}_{\mathcal{S}}$, interacts with a measurement apparatus A , described by basis vectors $\{|a_n\rangle\}$ spanning a Hilbert space \mathcal{H}_A , where the $|a_n\rangle$ are assumed to correspond to macroscopically distinguishable positions that correspond to the outcome of a measurement if \mathcal{S} is in the state $|s_n\rangle$. The dynamics of the quantum state of a quantum system is given by the Schrödinger equation. If \mathcal{S} is in a microscopical superposition of states $\sum_n c_n |s_n\rangle$, and A is in the initial "prepared" quantum state $|a_r\rangle$, the linearity of the Schrödinger equation entails that the total system $\mathcal{S}A$, assumed to be represented by the Hilbert product space $\mathcal{H}_{\mathcal{S}} \otimes \mathcal{H}_A$, evolves with time according to

$$\left(\sum_n c_n |s_n\rangle \right) \Big| a_r \rangle \rightarrow_t \sum_n c_n |s_n\rangle |a_n\rangle$$

where the coefficients c_n are some functions of time. This dynamical evolution is often referred to as a *preparation* procedure in order to emphasize that the process does not suffice to directly conclude that a measurement has actually been completed. A preparation procedure will be denoted by φ and a measurement effected by using some instrument will be denoted by A . The probability that the measurement gives rise to a value lying in the Borel set $E \subseteq \mathbb{R}$ will be denoted by $P[\varphi, A; E]$. The set of measurement is assumed to be discrete, indeed. Two different preparation procedures φ_1 and φ_2 such that the

corresponding probability distributions $P[\varphi_1, A; \cdot]$ and $P[\varphi_2, A; \cdot]$ are identical for any instrument A are said to be equivalent [2], $\varphi_1 \sim \varphi_2$. An equivalence class of procedures with respect to the defined equivalence relation is called a *state*, and the set of all states will be denoted by Σ . Similarly, if for two instruments A_1 and A_2 the probability distributions $P[\varphi_1, A; \cdot]$ and $P[\varphi_2, A; \cdot]$ agree for all states $\varphi \in \Sigma$ we call the instruments equivalent, $A_1 \sim A_2$, and the equivalence classes of this equivalence relation are called *observables*. The set of all observables will be denoted by \mathcal{D} . If any measurement of $A \in \mathcal{D}$ gives only positive results, $\varphi(A) \geq 0$, for any $\varphi \in \Sigma$, we call A positive, $A \geq 0$.

We further assume that \mathcal{D} can be embedded in a C^* -algebra \mathcal{A} , a complex algebra of continuous linear operators on a complex Hilbert space, which is a topologically closed set in the norm topology of operators and is closed under the operation of taking adjoints of operators. Then the observables correspond to the self-adjoint $A = A^*$ elements of \mathcal{A} . The states Σ are identified with the set of all continuous positive and normalized functionals on \mathcal{A} , $\Sigma \cong \{\varphi \in \mathcal{A}^* : \varphi(A^*A) \geq 0, \forall A \in \mathcal{A}, \varphi(\mathbb{I}) = 1\}$.

The (presumably reversible) time evolution of a closed quantum system described in a certain representation by a von Neumann algebra \mathcal{M} is given by a one-parameter group of $*$ -automorphisms $\{\alpha_t\}_{t \in \mathbb{R}}$ of \mathcal{M} . That is, each α_t is a bijective linear map on \mathcal{M} such that $\alpha_t(xy) = \alpha_t(x)\alpha_t(y)$ and $\alpha_t(x^*) = \alpha_t(x)^*$ for all $x, y \in \mathcal{M}$, and such that it satisfies the group property $\alpha_s \circ \alpha_t = \alpha_{s+t}$ for all $s, t \in \mathbb{R}$. Moreover, we shall assume that $t \mapsto \varphi(\alpha_t(x))$ is continuous for any normal state φ , and that expectation values move continuously in time – the so called *weak* continuity*.

6.2 Open systems and decoherence

We consider a subsystem of a closed physical system described by a von Neumann algebra \mathcal{N} containing the observables of the system, together with a reversible time evolution given by a weak* continuous one-parameter group $\{\alpha_t\}_{t \in \mathbb{R}}$ of $*$ -automorphisms. The subsystem will be described by a subalgebra $\mathcal{M} \subseteq \mathcal{N}$ which includes those observables pertaining to the subsystem. In addition we assume the existence of a normal conditional expectation $E : \mathcal{N} \rightarrow \mathcal{M}$, which is a weak* continuous linear and idempotent map of norm one. Then the reduced time evolution is defined by $T_t(x) = E \circ \alpha_t(x)$, $x \in \mathcal{M}$, $t \geq 0$. In general, the reduced time evolution is no longer reversible, reflected by the fact that the evolution operators T_t are noninvertible. The reduced time evolution $\{T_t\}_{t \geq 0}$ is a completely positive linear map for every $t \geq 0$, with $\|T_t\| \leq 1$, and $t \mapsto T_t(x)$ is ultraweakly continuous for all $x \in \mathcal{M}$.

The reduced dynamics $\{T_t\}_{t \geq 0}$ is said to display *decoherence* if there is a decomposition $\mathcal{M} = \mathcal{M}_1 \oplus \mathcal{M}_2$ such that for every observable $x \in \mathcal{M}$ there exist a unique decomposition into self-adjoint operators $x_1 \in \mathcal{M}_1$ and $x_2 \in \mathcal{M}_2$ such that $x = x_1 + x_2$, and $\lim_{t \rightarrow \infty} \varphi(T_t(x_2)) = 0$, for all normal states φ , i.e. all expectation values of x_2 converge to 0 as time tends to infinity, so that \mathcal{M}_2 part is beyond experimental resolution after decoherence has taken place. Thus, in the limit $t \rightarrow \infty$ the system behaves effectively (and therefore valid for all practical purposes) like a closed system described by the von Neumann algebra of effective observables \mathcal{M}_1 with reversible time evolution given by the one-parameter group $\{\beta_t\}_{t \in \mathbb{R}}$. We summarize the algebraic framework in the following

diagram.

$$\begin{array}{ccc}
\mathcal{N} & \xrightarrow{\{\alpha_t\}_{t \in \mathbb{R}}} & \mathcal{N} \\
E \downarrow & & \downarrow E \\
\mathcal{M}_1 \oplus \mathcal{M}_2 & \xrightarrow{\{T_t\}_{t \geq 0}} & \mathcal{M}_1 \oplus \mathcal{M}_2 \\
t \rightarrow \infty \downarrow & & \downarrow t \rightarrow \infty \\
\mathcal{M}_1 & \xrightarrow{\{\beta_t\}_{t \geq 0}} & \mathcal{M}_1
\end{array} \tag{43}$$

The time evolution of observables contained in the von Neumann algebra \mathcal{N} is described by the weak* continuous one-parameter group of *-automorphisms $\{\alpha_t\}_{t \in \mathbb{R}}$. Then, under the action of the conditional expectation E , the dynamics is reduced to a completely positive linear map $\{T_t\}_{t \geq 0}$. And, for all practical purposes, in the limit $t \rightarrow \infty$, the decoherent system can be considered as a closed system described by the von Neumann algebra of effective observables \mathcal{M}_1 with reversible time evolution given by the one-parameter group $\{\beta_t\}_{t \in \mathbb{R}}$.

It is remarkable that the quantum decoherence diagram shown above constitutes nothing else but a quantum mechanical version of the diagram shown in Figure 1, representing multi-level systems schematically. In fact, our diagram has two levels – quantum and classical – instead of the single classical level of the previous sections. Namely, we have shown that a subsystem of a closed physical system described by a von Neumann algebra \mathcal{N} containing the observables of the system, with a reversible time evolution given by a weak* continuous one-parameter group of automorphisms, can be described by a reduced dynamics – represented by the new set of "macro-variables" analogous to Y in the diagram in Figure 1 – which is said to display decoherence if there is a decomposition of observables into a direct sum of self-adjoint operators belonging to the classical and quantum subalgebras, and all expectation values of the quantum part converge to 0 as time tends to infinity.

It is also remarkable that our diagram resolves the conundrum question related to the Kochen-Specker (KS) theorem. KS proves that there is a contradiction between two basic assumptions of the hidden variable theories intended to reproduce the results of quantum mechanics: that all hidden variables corresponding to quantum mechanical observables have definite values at any given time, and that the values of those variables are intrinsic and independent of the device used to measure them. This contradiction is caused by the fact that quantum mechanical observables need not be commutative, so that it turns out to be impossible to simultaneously embed all the commuting subalgebras of the algebra of these observables in one commutative algebra, assumed to represent the classical structure of the hidden variables theory, if the Hilbert space dimension is at least three. We overcome and explain the paradox by showing that all expectations of the non-commutative components corresponding to quantum mechanical observables vanishes with time – and, in infinite time, only commutative, classical observables can be measured in the macroscopic world.

Furthermore, by looking at the structure of the von Neumann algebra of effective observables \mathcal{M}_1 and the evolution $\{\beta_t\}_{t \in \mathbb{R}}$, we may classify different scenarios of decoherence.

6.3 Scenarios of decoherence

In the following list we briefly introduce possible scenarios that can emerge due to decoherence skipping the details for [13].

If the von Neumann algebra of effective observables \mathcal{M}_1 is commutative and $\{\beta_t\}_{t \in \mathbb{R}} = \text{id}$ for all t , then we speak of environmentally induced *pointer states*. This situation is characteristic for a measuring apparatus, where the von Neumann algebra of effective observables \mathcal{M}_1 contains the observables representing the pointer positions of the apparatus. The commutativity ensures that we obtain a classical probability distribution over the pointer positions whereas the triviality of $\{\beta_t\}_{t \in \mathbb{R}}$ ensures that the pointer observables are immune to the interaction with the environment.

If the von Neumann algebra of effective observables \mathcal{M}_1 is noncommutative but has a nontrivial center – the set of all those elements that commute with all other elements – we speak of environmentally induced *superselection rules*. Then the center of algebra contains the superselection observables which are classical observables, taking a definite value in each sector.

If the von Neumann algebra of effective observables \mathcal{M}_1 is a factor algebra again, then after decoherence the system effectively behaves like a closed system with evolution $\{\beta_t\}_{t \in \mathbb{R}}$, still having a pure *quantum character*. However, it may be smaller than the original system.

If the von Neumann algebra of effective observables \mathcal{M}_1 is commutative, we speak of an environment induced *classical structure*. Then the system can effectively be described in terms of classical probability. However, a classical physical system has more structure. For example, the underlying classical probability space and the time evolution, given by $\{\beta_t\}_{t \in \mathbb{R}}$, need not come from a classical dynamical system, or more precisely, from the Hilbert space representation of a topological or smooth classical dynamical system with a evolution given by a flow on phase space Ω .

Finally, if the von Neumann algebra of effective observables \mathcal{M}_1 is a constant (a number on its own), the system is ergodic.

7 Conclusion

The study of multi-level systems is a challenging endeavor in many ways, from data collection and modeling to analysis and control. The individual sections of the present article form a sample of quite different examples coming from various application areas. Through these examples we have, on the one hand, aimed to point out the difficulties in constructing a general theory of multi-level systems, while on the other hand we have maintained that a common foundation may be possible upon which such a theory can be built.

It is hoped that the various perspectives presented here will be useful for a common framework in the discussion of multi-level structures within and across different scientific disciplines.

As discussed in the introduction, the main interest of developing multi-level description of systems is, on the one hand, to simplify the description in the sense of reducing the number of degrees of freedom, and on the other hand, and more fundamentally, to extract from this reduction some emerging principles that were not visible at the initial level. A similar process has occurred several times in the history of physics with e.g. the development of electromagnetism or statistical physics. Certainly, the dream of extracting generic laws of nature in economics, sociology, neuroscience, in the same way as physics

did, is part of the motivation for developing multi-level descriptions.

However, there exists strong and structural differences with physical systems. First, when dealing with multi-agents, neuronal systems, economic actors, etc., the nature of interactions is quite different from physics: they are not symmetric, they depend on a possibly very long history (memory), and they can even display a form of anticipation of the future as well as different degrees of expectation (e.g. expectation of expectation [9]). Additionally, evolution is usually irreversible and non-stationary. As a consequence, the usual wisdom coming from physics may not be directly applicable to these systems, and the emerging principles (if any) can be quite different.

As the main goal of studying these systems via mathematics is to propose a set of equations that can be analyzed (analytically or numerically) so as to lead to explanations and predictions, one is trying to reduce the complexity of the initial system by reducing the number of degrees of freedom, e.g., by changing the level of description. However, one must be careful: as the analytical (not to speak of rigorous) derivation, as well as the analysis of the higher level equations are complex, one might be tempted to propose ad hoc simplifications that lose some important features of the emerging dynamics. There is therefore a trade-off between what we are able to achieve with the model at hand (i.e. which techniques we have to solve it) and how much it is realistic or predictive (i.e. how to validate the model). These questions are obviously common to any modelling problem, but we would like to focus here on the content of this paper and what we have learned. Let us first focus on the main problems raised from multi-scale approaches and the mathematical tools are available to solve them.

First, the information-theoretic tools described in Section 2 allow to identify whether the induced dynamics (Y, ψ) at a *given* higher level of description is closed in the sense that the dynamics of the observable(s) associated to Y is a function of these observables only. This is particularly interesting, as a given application problem is usually related to certain specific aggregate quantities that hence define Y . In physics, for instance, observables usually emerge naturally from the phenomenological knowledge of the system, although in systems such as, e.g., spin glasses, the definition of these observables is not straightforward. In the context of agent-based models, to recall the example addressed in Section 3, observables of interest are in many (though not all) cases related to aggregations over agent attributes and this defines an associated state space Y . While in Section 2 the information-theoretic tools were developed in a finite-state, discrete-time setting, it can be extended also to continuous states and time— see [?] for an example. Their application to the mean-field neuronal dynamics might reveal a relation between the history dependence of the derived covariance term and the information flow across levels.

As we have seen, going to a higher level is meant to reduce the number of degrees of freedom, but this does not necessarily mean that what we have obtained is simpler: the difficulty might be displaced and there might be a price to pay. We have seen, for example, that the change of level can lead a Markovian system to a non-Markovian one. Which methods do we have to handle systems with a virtually infinite memory? A simple case occurs when correlation decay is exponential as in Section 4; in this case one can propose a Markovian approximation by cutting the memory beyond the time scale of correlation decay. Another option can be to refine the level of observation in accordance with the relevant model symmetries, as seen in Section 3. More generally, tools exist in the field of probability theory (variable length Markov chains, chains with complete connections) or statistical physics (Gibbs distributions). Note that the concept of Gibbs distributions allowing left and right conditioning (i.e., on the past and on the future) could be a proper

setting to model anticipation mechanisms as well. They can also handle non-stationary problems.

A different and more complicated problem arises if the higher-level state space Y is not given a priori and the task is to find those quantities (observables) which best characterise the dynamical behaviour of the system. It may be possible to identify quantities for which the dynamics are closed (such as for the specific sub-population structures in Sections 3 and 4), but generally, in more realistic settings, every considerable dimensionality reduction will go with a loss of precision in relation to the original dynamics. This leads to the question of how such approximations should be evaluated, which generally has to deal with a trade-off between accuracy of the approximate description in relation to its complexity (and the mathematical solution tools available). Notice that, for agent-based systems, this problem has been addressed in [?]. For instance, when dealing with neuron populations it is not necessarily sufficient to characterize firing rates of all neurons simultaneously, as neurons may have also spatio-temporal correlations which are not explained by rates. But then, the question is which correlations? Is it sufficient to include pairwise correlations, or do we have to go to higher order to explain the dynamics? This is again associated with the definition of the space Y in Figure 1. However, if the higher-level dynamics ψ is not the induced dynamics from the micro-level process, the closure measures described in Section 2 are not the appropriate tools to evaluate their quality. Thus, the development of suitable methods to deal with this problem will be a topic of future research.

reduction exists, it is closely related to the system under consideration. In physics, observable usually naturally emerge from the phenomenological knowledge of the system, although in systems such as e.g. spin glasses, the definition of these observables is not straightforward. In systems coming from neuroscience, sociology, economics, the situation is even worse especially as it is difficult to find a set of observables that allows a prediction of the system behaviour. For example, in neuroscience,

Acknowledgement. The research leading to these results has received funding from the European Union’s Seventh Framework Programme (FP7/2007-2013) under grant agreement no. 318723: *Mathematics of Multi-Level Anticipatory Complex Systems* (Math-eMACS). S.B. also acknowledges financial support by the Klaus Tschira Foundation. D.V. acknowledges the support from the Cluster of Excellence Cognitive Interaction Technology ‘CITEC’ (EXC 277) at Bielefeld University, which is funded by the German Research Foundation (DFG).

References

- [1] S. Amari. Characteristics of random nets of analog-like elements. *IEEE Trans. Syst. Man and Cybernetics.*, SMC-2(5):643–657, 1972.
- [2] H. Araki. *Mathematical Theory of Quantum Fields*. Oxford University Press, 1999.
- [3] F. M. Atay and L. Roncoroni. Exact lumpability of linear evolution equations in Banach spaces. *MPI-MIS Preprint Series*, 109/2013. <http://www.mis.mpg.de/publications/preprints/2013/prepr2013-109.html>.
- [4] R. Axelrod. The Dissemination of Culture: A Model with Local Convergence and Global Polarization. *The Journal of Conflict Resolution*, 41(2):203–226, 1997.

- [5] S. Banisch. The probabilistic structure of discrete agent-based models. *Discontinuity, Nonlinearity, and Complexity*, 3(3):281–292, 2014. <http://arxiv.org/abs/1410.6277>.
- [6] S. Banisch. *Markov Chain Aggregation for Agent-Based Models*. Understanding Complex Systems. Springer, 2015 (in press).
- [7] S. Banisch and R. Lima. Markov Chain Aggregation for Simple Agent-Based Models on Symmetric Networks: The Voter Model. *Advances in Complex Systems*, 18(03n04):1550011, 2015. arxiv.org/abs/1209.3902.
- [8] S. Banisch, R. Lima, and T. Araújo. Agent based models and opinion dynamics as Markov chains. *Social Networks*, 34:549–561, 2012.
- [9] M. Barber, P. Blanchard, E. Buchinger, B. Cessac, and L. Streit. A luhmann-based model of communication, learning and innovation. *Journal of Artificial Societies and Social Simulation*, 9(4), 2006.
- [10] M. L. Bellac. *Quantum and Statistical Field Theory*. Oxford, Clarendon Press, 1991.
- [11] G. Ben-Arous and A. Guionnet. Large deviations for langevin spin glass dynamics. *Probability Theory and Related Fields*, 102(4):455–509, 1995.
- [12] P. Blanchard and M. Hellmich. Decoherence in infinite quantum systems. *Quantum Africa 2010: Theoretical and Experimental Foundations of Recent Quantum Technology*, AIP Conf. Proc. 1469:2–15, 2012.
- [13] P. Blanchard and R. Olkiewicz. Decoherence induced transition from quantum to classical dynamics. *Rev. Math. Phys.*, 15:217–243, 2003.
- [14] J. P. Bouchaud, L. F. Cugliandolo, J. Kurchan, and M. Mézard. Mode-coupling approximations, glass theory and disordered systems. *Physica A*, 226:243–273, 1996.
- [15] B. Cessac. Occurrence of chaos and AT line in random neural networks. *Europhys. Lett.*, 26(8):577–582, 1994.
- [16] B. Cessac. Increase in complexity in random neural networks. *J. de Physique*, 5:409–432, 1995.
- [17] B. Cessac, B. Doyon, M. Quoy, and M. Samuelides. Mean-field equations, bifurcation map, and route to chaos in discrete time neural networks. *Physica 74 D*, pages 24–44, 1994.
- [18] T. Cover and J. Thomas. *Elements of Information Theory*. Wiley-Interscience, New York, 1991.
- [19] E. Daucé, M. Quoy, B. Cessac, B. Doyon, and M. Samuelides. Self-organization and dynamics reduction in recurrent networks: stimulus presentation and learning. *Neural Networks*, 11:521–33, 1998.
- [20] O. Faugeras and J. M. Laurin. A large deviation principle for networks of rate neurons with correlated synaptic weights. *arXiv*, 1302.1029, 2013.
- [21] O. Faugeras, J. Touboul, and B. Cessac. A constructive mean field analysis of multi population neural networks with random synaptic weights and stochastic inputs. *Frontiers in Computational Neuroscience*, 3(1), 2009.

- [22] W. Freeman. *Mass Action in the Nervous System*. Academic Press, New York, 1975.
- [23] D. Geiger, T. Verma, and J. Pearl. Identifying independence in bayesian networks. *Networks*, 20(5):507–534, 1990.
- [24] S. Geman. Almost sure stable oscillations in a large system of randomly coupled equations. *SIAM J. Appl. Math.*, 42(4):695–703, 1982.
- [25] N. I. Gillespie and C. E. Praeger. Neighbour transitivity on codes in hamming graphs. *Designs, codes and cryptography*, 67(3):385–393, 2013.
- [26] L. Horstmeyer and F. M. Atay. Characterization of exact lumpability of smooth dynamics on manifolds. *MPI-MIS Preprint Series*, 70/2015. <http://www.mis.mpg.de/publications/preprints/2015/prepr2015-70.html>.
- [27] B. H. Jansen and V. G. Rit. Electroencephalogram and visual evoked potential generation in a mathematical model of coupled cortical columns. *Biological Cybernetics*, 73:357–366, 1995.
- [28] J. G. Kemeny and J. L. Snell. *Finite Markov Chains*. Springer, 1976.
- [29] A. V. L.Ts. Adzhemyan, N.V. Antonov. *The Field Theoretic Renormalization Group in Fully Developed Turbulence*. Gordon and Breach, 1999.
- [30] L. Molgedey, J. Schuchardt, and H. Schuster. Suppressing chaos in neural networks by noise. *Physical Review Letters*, 69(26):3717–3719, 1992.
- [31] O. Moynot and M. Samuelides. Large deviations and mean-field theory for asymmetric random recurrent neural networks. *Probability Theory and Related Fields*, 123(1):41–75, 2002.
- [32] J. Naudé, B. Cessac, H. Berry, and B. Delord. Effects of cellular homeostatic intrinsic plasticity on dynamical and computational properties of biological recurrent neural networks. *Journal of Neuroscience*, 33(38):15032–15043, Oct. 2013.
- [33] O. Pfante, E. Olbrich, N. Bertschinger, N. Ay, and J. Jost. Closure measures for coarse-graining of the tent map. *Chaos: An Interdisciplinary Journal of Nonlinear Science*, 24(1):013136, 2014.
- [34] O. Pfante, E. Olbrich, N. Bertschinger, N. Ay, and J. Jost. Comparison between different methods of level identification. *Advances in Complex Systems*, 17(2):1450007, 2014.
- [35] T. Schelling. Dynamic Models of Segregation. *Journal of Mathematical Sociology*, 1(2):143–186, 1971.
- [36] H. Sompolinsky, A. Crisanti, and H. Sommers. Chaos in random neural networks. *Physical Review Letters*, 61(3):259–262, 1988.
- [37] H. Sompolinsky and A. Zippelius. Relaxational dynamics of the Edwards-Anderson model and the mean-field theory of spin-glasses. *Physical Review B*, 25(11):6860–6875, 1982.

- [38] A. Vasiliev. *The field theoretic renormalization group in critical behavior theory and stochastic dynamics*. Chapman and Hall / CRC, 2004.
- [39] D. Volchenkov. Renormalization group and instantons in stochastic nonlinear dynamics: From self-organized criticality to thermonuclear reactors. *European Physical Journal - Special Topics 1951-6355*, 170(1):1–142, 2009.
- [40] H. Wilson and J. Cowan. Excitatory and inhibitory interactions in localized populations of model neurons. *Biophys. J.*, 12:1–24, 1972.
- [41] J. Zinn-Justin. Renormalization and renormalization group: From the discovery of uv divergences to the concept of effective field theories. *Proceedings of the NATO ASI on Quantum Field Theory: Perspective and Prospective*. In: de Witt-Morette C., Zuber J.-B. (eds), Kluwer Academic Publishers, NATO ASI Series C 530:375–388, 1999.
- [42] J. Zinn-Justin. *Quantum field theory and critical phenomena*. Oxford, Clarendon Press, 2002.